JOURNAL OF Applied Polymer SCIENCE

Agricultural residue-derived lignin as the filler of polylactic acid composites and the effect of lignin purity on the composite performance

Yiwei Gao,[1*] Wangda Qu,[1*] Yang Liu,[2] Hui Hu,[2] Eric Cochran,[3] Xianglan Bai[1]
[1]Department of Mechanical Engineering, Iowa State University, Ames, Iowa 50011
[2]Department of Aerospace Engineering, Iowa State University, Ames, Iowa 50011
[3]Department of Chemical and Biological Engineering, Iowa State University, Ames, Iowa 50011
Correspondence to: X. Bai (E-mail: bxl9801@iastate.edu)

ABSTRACT: In this study, corn stover lignin with different purities was used as filler in polylactic acid (PLA) matrix. It was found that the impurity metals present in unpurified lignin can significantly affect the performance of the composites in terms of their thermal stability, rheological behavior, mechanical properties, and hydrophobicity. Among the PLA composites, the ones fabricated with the lignin containing 4% of impurities overall had the best thermal stability and tensile strength. From melt rheology analysis, it was also found that the presence of the impurity metals decreases the complex viscosity of the composites. It is suggested that the impurity metals acted as catalysts to promote the interaction between lignin and PLA, resulting in an improved compatibility between PLA and the filler. In the present study, mechanical properties and hydrophobicity of the composites were further improved by acetylating the lignin with the optimum content of impurities. Tensile strength of the composite with the acetylated lignin was comparable to that of pure PLA, whereas the modulus increased to as high as 2.75 GPa. Overall, the study showed that unpurified lignin could be used as filler to achieve similar or better performance than the composites made with highly purified lignin fillers. © 2019 Wiley Periodicals, Inc. J. Appl. Polym. Sci. **2019**, *136*, 47915.

KEYWORDS: biodegradable; composites; mechanical properties; rheology; thermal properties

Received 8 October 2018; accepted 5 April 2019
DOI: 10.1002/app.47915

INTRODUCTION

Lignin is known as the most abundant aromatic polymer in nature, present in most terrestrial plants with weight percentages from 15 to 40%.[1] Lignin was traditionally produced from pulp and paper industries as a byproduct. In recent years, an increasing amount of lignin is also generated from emerging bio-refineries, derived from various biomass, including both woody and non-woody biomass, such as agricultural residues and energy grasses.[2] It is estimated that the annual lignin production will reach 220 million tons by the year of 2030.[3] Although the majority of lignin is currently burned for heat and power generation, value-added applications of lignin have gained great attention in recent years due to the abundancy of lignin at low cost and the need for improving economic sustainability of the biorefineries. For instance, lignin has been converted to biofuels and chemicals or applied to materials such as engineered plastics, composites, polymers, and carbon fiber.[4–7]

Lignin can be used as filler in polymers. Lignin filler could not only reduce material costs but also potentially alter the properties of the parent materials. For example, Chen et al. and Canetti *et al.*[8,9] reported that lignin fillers could raise the thermal degradation temperature of polypropylene. Baumberger *et al.*[10] reported that lignin could reduce the water affinity of starch films, owing to the hydrophobicity of lignin. Gordobil *et al.*[11,12] found that using a low concentration of lignin as filler increases the strain of the composites. Using lignin as fillers in polylactic acid (PLA) is particularly attractive as both materials are biobased and biodegradable. In the previous studies, mostly woody biomass-derived Kraft and alkali lignin were applied as filler.

Although it varies depending on the biomass source and lignin isolation process, as-received technical lignin could contain considerable amounts of inorganic impurities, which can be over 10%.[12] The origins of the impurities include inorganic elements intrinsically bonded to plant cells and chemicals added during lignin isolation process. Thus, lignin was often purified to remove impurities before it was further upgraded.[11] However, lignin purification is a tedious and costly process, which therefore can greatly diminish the low-cost advantage of lignin. In addition, the acid-washing for lignin purification potentially raises the need for wastewater treatment. Thus, using as-received lignin or the lignin with minimal purification would be

*Co-first authors.

highly desired from economic and environmental perspectives. However, the possible effects of the unremoved impurities on the filler performance and composite properties are unclear. It is well known that indigenous alkaline and alkaline earth metals present in plants can influence biomass pyrolysis through their catalytic effects.[13]

In this study, corn stover-derived organosolv lignin with different contents of inorganic impurities were used as fillers in PLA matrix. Corn stover is the most abundant agricultural residue in the United States, and its production is estimated to be 200~250 million dry tons per year.[14] Corn stover is also the popular feedstock in biorefineries in the United States. Thus, corn stover-derived lignin is one of the major byproducts in the biorefineries. It is also noteworthy that compared to woody-biomass derived lignins, herbaceous biomass-based lignin (such as corn stover lignin) has lower thermal stability and higher chemical reactivity due to its higher content of phenolic hydroxyl and branched aliphatic side chains.[15] The aims of the present study are two folds: to investigate the role of the lignin impurities on the composite performance and evaluate the potential of the agricultural-residue lignin in filler application.

EXPERIMENTAL SECTION

Materials

Corn stover derived organosolv lignin was provided by the Archer Daniels Midland (ADM) Company. PLA was purchased from NatureWorks (6260D), and acetic anhydride (99%) and pyridine (99%) were from Fisher Scientific. Hydrochloric acid was purchased from Sigma Aldrich.

Lignin Purification

As-received lignin was dissolved in 0.1 N hydrochloric acid and stirred continuously to remove acid-soluble inorganic impurities. The lignin was then repeatedly rinsed with deionized water, followed by drying in a vacuum oven at 40 °C overnight. Three kinds of lignin with varied inorganic contents were obtained and used in the present study. Lignin purity was controlled by varying the number of rinsing cycles. Lignin was stirred vigorously during the rinsing and each cycle was lasted for 0.5 h. Based on the inorganic content, the lignin was designated as H-lignin (high inorganic content, also the as-received lignin), M-lignin (medium inorganic content, one rinsing cycle), and L-lignin (low inorganic content, three rinsing cycles).

Acetylation of Lignin

Lignin acetylation was performed following a laboratory-developed protocol. In general, 5 g of M-lignin was acetylated with 50 mL of solution consisting of acetic anhydride and pyridine at 1:1 (v/v) ratio at room temperature for 24 h. The acetylated lignin was precipitated from the solution by adding excess amount of methanol. The precipitated lignin was then washed with deionized water three times, followed by drying in the vacuum oven overnight.

Preparation of PLA–Lignin Composite Films

PLA and H-lignin, M-lignin, or L-lignin were blended in a twin-screw micro-compounder (DACA Instruments, Santa Barbara, CA) at 200 °C. Each kind of lignin was mixed with PLA at 5, 10, and 15% of filler concentrations. The rotation speed of the screws was 200 rpm, and the composites were mixed for 15 min before extrusion. About 2 g of the extruded PLA–lignin composites were hot-pressed by a Carver furnace at 200 °C for 30 s with the applied force of 1 metric ton to form films with thickness of 0.02 mm. The PLA–lignin composites with different kinds of lignin fillers are denoted as PLA–L-lignin, PLA–M-lignin, and PLA–H-lignin. Other symbols were also used to specify both the lignin type and lignin filler concentration. For example, PLA-L5 stands for the composite containing 5% of L-lignin.

Characterizations

Total inorganic content in lignin was determined using a Mettler Toledo TGA/DSC system. About 10 mg of lignin sample was heated from room temperature to 900 °C at 10 °C/min under nitrogen environment. After the sample was kept at 900 °C for 30 min, air was introduced to burn off the residue solid. The remaining non-combustible solid is total inorganic impurities. The inorganic composition was also determined by analyzing lignin using Inductively Coupled Plasma Optical Emission Spectrometer (ICP-OES) (Optima 8000, PerkinElmer). Lignin samples were digested first using an Anton Paar Microwave Digester Multiwave 3000 (Graz, Australia). The samples were prepared by adding approximately 500 mg of lignin and 10 mL of nitric acid to the quartz digestion reactor vessel. The microwave digestion was programmed according to Environmental Protection Agency (EPA) method 3051A to a temperature of 180 ± 5 °C. Elemental composition of lignin was also analyzed using Elementar (vario MICRO cube) elemental analyzer. During the analysis, approximately 5 mg of sample was combusted at 900 °C, and the combustion products, carbon dioxide, water, and nitric oxide were characterized by a thermal conductivity detector. The weight percentages of the C, H, and N were calculated based on the amount of the combustion products.

Thermal stability of lignin or PLA–lignin composites was determined using the same TGA/DSC system. About 10 mg samples were heated from room temperature to 600 °C at 10 °C/min with a nitrogen flow rate of 100 mL/min.

To confirm acetylation, the particles of lignin and acetylated lignin were analyzed by Fourier transform infrared (FTIR) analysis. FTIR analysis was conducted using a Thermo Scientific Nicolet iS10 (Thermo Fisher Scientific Inc., Waltham, MA) equipped with a Smart iTR accessory. The wave numbers of the FTIR analysis ranged from 750 to 4000 cm^{-1}, and each sample was scanned 32 times at a resolution of 4 cm^{-1} and interval of 1 cm^{-1}.

All the above analyses were at least duplicated.

To measure wettability, a deionized water droplet was placed on the surface of the PLA/lignin composite film. The images of the water droplet on the film were captured by a high-speed camera (Fastcam Mini WX100, PCO) with a 12× zoom lens system (LaVision). The contact angle was measured by processing the image using PFV software (Ver.3670). The reported results were averages of at least three tests at 95% confidence interval.

Rheology measurements of the composites were performed using a Discovery hybrid rheometer (DHR-2, TA Instruments) with 25 mm parallel-plate geometry. Samples were trimmed at a gap of 1050 μm before conducting the test with a 1000 μm gap. Dynamic frequency sweep (0.1 rad/s to 100 rad/s) was conducted

at 200 °C with strain of 1.25%. For temperature sweep, the sample was heated from 150 to 200 °C at 10 rad/s and a strain of 1.25%.

Mechanical properties of the composite films were measured using the same rheometer with dynamic mechanical analysis (DMA) clamps. A modified method was used based on ASTM D 53455. The films with 5 mm width and 40 mm length were fixed to the clamps with a gap of 25 mm and stretched at 5 mm/min until break. The reported values were averages of at least 10 tests.

The optical micrograph of the composite films was observed using a Leica DM IL LED microscope, and the images were recorded by a camera. The most representative image was shown for each case.

RESULTS AND DISCUSSION

Lignin Characterization

As shown in Table I, the contents of the inorganic impurities were 2% for L-lignin, 4% for M-lignin, and 7% for H-lignin. From ICP analysis (Figure 1), various inorganic elements, including Al, Ca, Fe, Mg, Mn, P, S, Na, and K, were detected from H-lignin. Sulfur and phosphorus were also found, probably in the form of sulfate and phosphate. In comparison to H-lignin, the amounts of alkali metals (Na, K), alkaline earth metals (Ca, Mg), and P decreased in M-lignin. In addition, the content of Al and Fe also decreased. L-lignin contained least amounts of inorganic metals although the elements of Al, Ca, Fe, K, and Mg were still detectable from the lignin. The amount of sulfur was relatively constant among the different kinds of lignin, implying that sulfate is not easily washed away by acid washing. Sulfur is also prone to form lignin sulfonates that are harder to remove. It was difficult to remove the inorganic content to below 2% even after rigorous washing because of the silicate content in lignin.[16] Silicate is not detectable by ICP due to its poor acid solubility. Because silicates cannot be removed by acid washing, the difference in the impurity concentrations among the three kinds of lignin was due to the variations in their inorganic metal contents.

The result of the elemental analysis is also given in Table I. The amount of carbon was 54.30% for H-lignin and increased to 58.06% for M-lignin, and 59.07% for L-lignin due to the removal of the inorganics. The contents of N, H, S, and O were relatively constant among the three kinds of lignin.

Thermal stability of the lignin is compared in Table II. The temperature corresponding to a 5% mass loss is defined as T_d, and T_{max} represents the temperature at which the rate of mass loss reaches maxima. The T_d's of the lignin were varied from 180 to 200.7 °C for the three kinds of lignin, decreasing with increasing inorganic content in the lignin. The T_d of corn stover lignin measured in this study was lower than that of softwood alkali lignin

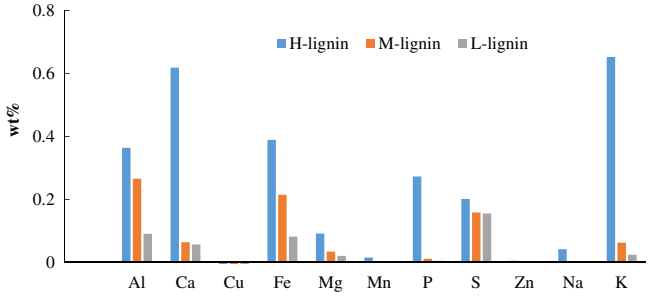

Figure 1. ICP analysis of lignin. [Color figure can be viewed at wileyonlinelibrary.com]

reported by Gordobil *et al.*,[12] possibly attributed to the longer aliphatic side chains attached to aromatic rings.[15] The range of T_{max} was between 335.5 and 350.3 °C for different corn stover lignin, which also decreased with increasing inorganic content. Lower T_d and T_{max} correspond to lower thermal stability of lignin. Thermal stability of lignin decreased with increasing inorganic content because the metal elements can catalyze lignin decomposition during heating. Usually, alkaline metals have stronger catalytic effect compared to alkaline earth metals.[17] As shown in Table II, the yields of (ash-free) char residue decreased with increasing inorganic content in lignin due to enhanced catalytic cracking and increased devolatilization. Although silicates also present in lignin, they are inert and do not contribute to the catalytic effect. Moreover, their contents remain the same in all the lignin. Thus, the observed differences must be due to their different metal contents.

Properties of PLA–Lignin Composites

Thermal Stability. The T_d and T_{max} values of PLA and the PLA–lignin composites are listed in Table III. The T_d and T_{max} of pure PLA were 313.3 and 354 °C, both higher than that of lignin. Although lignin by itself had lower thermal stability than PLA, six of nine PLA–lignin composites had better thermal stability compared to pure PLA. Previously, Gordobil *et al.* also reported that PLA composites prepared with woody-biomass derived lignin fillers have similar thermal stability.[12] In the present study, thermal

Table II. Thermal Stability of Lignin Based on TGA Results

Lignin	T_d (°C)	T_{max} (°C)	Char residue (%)[a]
L-lignin	200.7	350.3	39.1
M-lignin	191.0	342.0	36.2
H-lignin	180.0	335.5	34.4

[a] Ash-free basis.

Table I. Inorganic Impurity Content and Elemental Composition in Lignin

Lignin	Inorganic impurities (%)	C (%)	H (%)	O (%)[a]	N (%)	S (%)
L-lignin	2.0	59.07	4.84	32.45	1.49	0.15
M-lignin	4.0	58.06	5.08	31.28	1.43	0.15
H-lignin	7.0	54.30	4.81	32.40	1.29	0.20

[a] By difference.

Table III. Thermal Stability of PLA and PLA–Lignin Composites

Composite	T_d (°C)	T_{max} (°C)
PLA	313.3	354.0
PLA-L5	313.8	357.2
PLA-L10	303.5	349.7
PLA-L15	304.7	352.5
PLA-M5	323.7	364.2
PLA-M10	316.5	358.8
PLA-M15	317.3	360.5
PLA-H5	318.7	362.3
PLA-H10	319.7	362.2
PLA-H15	310.2	355.0

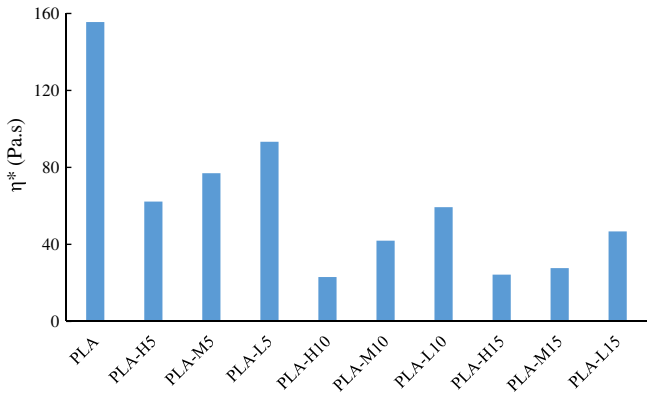

Figure 2. Complex viscosity η^* of PLA and PLA–lignin composites (T = 200 °C). The viscosity values stayed constants at angular frequency up to100 rad/s. [Color figure can be viewed at wileyonlinelibrary.com]

stability of the composites was correlated to both lignin concentration and impurity content. Among the nine composites, all PLA–M-lignin composites showed better thermal stability than pure PLA regardless their lignin concentration. For PLA–H-lignin, PLA-H5 and PLA-H10 showed improved T_d's compared to pure PLA. Further increasing lignin concentration resulted in a lower T_d in PLA-H15 compared to pure PLA. Unexpectedly, PLA–L-lignin composites had the lowest thermal stability; the T_d's of PLA-L10 and PLA-L15 were both noticeably lower than the T_d of pure PLA. The results indicate that the impurity metals in lignin actually promoted thermal stability of the PLA composites. As described above, thermal stability decreased by the presence of the impurity metals if lignin alone was pyrolyzed. Thus, the plausible explanation for the increased thermal stability in PLA–lignin composites could be that there form thermally stable intermolecular bonds between PLA and lignin. The impurity metals can catalyze lignin fragmentation and depolymerization during the thermal compounding. Due to the formations of new functional groups and free radicals at the bond cleaving ends, the lignin fragments would have much higher reactivity than parent lignin. These reactive species could further react with the PLA to form new intermolecular bonds. For example, the condensation reaction between phenolic OH of lignin fragments and the end chain OH in PLA could form stable aromatic C—O linkage. However, thermal stability of the composite did not monotonically increase with increasing metal content as PLA–M-lignin composites had better thermal stability than PLA–H-lignin composites. Excessively high content of metal content is undesired, because decomposition and devolatilization of the composites could occur at lower temperatures due to stronger catalytic cracking.

Rheological Properties. The processability of the composite during compounding is closely related to its rheological properties. Previously, the melt rheology of PLA blended with LDPE[18] or cellulose[19] was reported. However, rheological behavior of PLA–lignin composites was seldom found in literature. Figure 2 shows the complex viscosity of the composites measured at 200 °C. Lower viscosities of the composites would be favorable for uniform blending of the polymer and filler during extrusion. A lower zero-shear viscosity is beneficial to melt processing of the composite. Both PLA and the PLA–lignin composites showed Newtonian flow behavior at

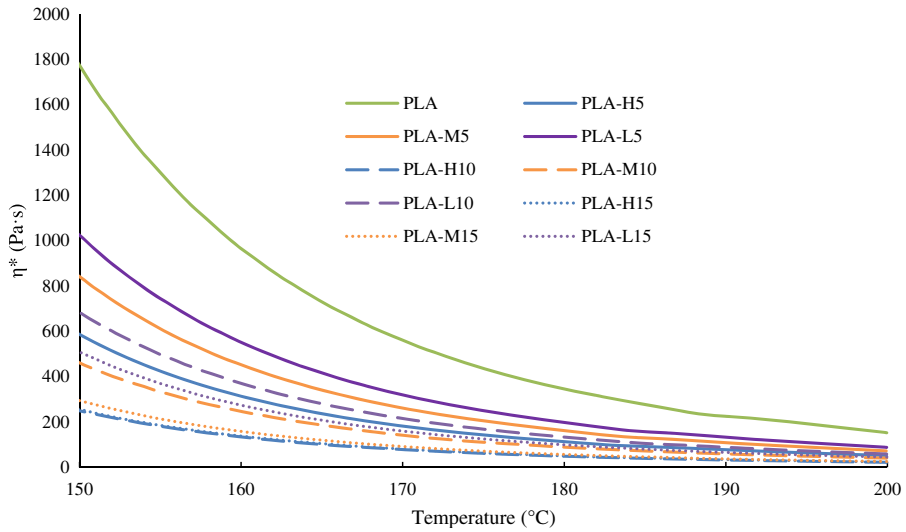

Figure 3. Complex viscosity η^* as a function of temperature for PLA and PLA–lignin composites (angular frequency ω = 10 rad/s). [Color figure can be viewed at wileyonlinelibrary.com]

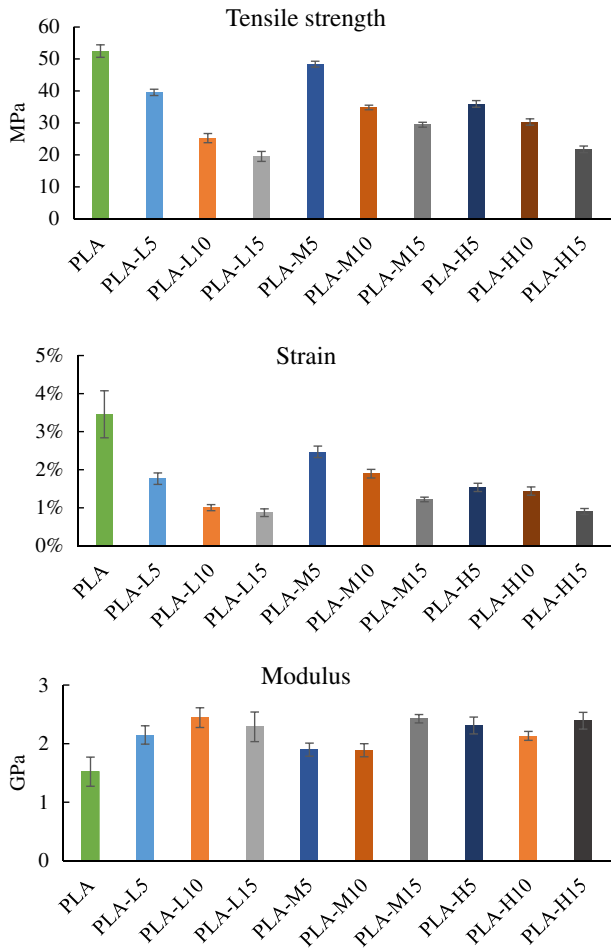

Figure 4. Mechanical properties of PLA and PLA–lignin composites. [Color figure can be viewed at wileyonlinelibrary.com]

the entire angular frequency range (up to 100 rad/s), as the viscosity values were independent with the frequency change. It was also found that the viscosities of the composites were lower than the viscosity of pure PLA and decreased with increasing lignin concentration in the composites. For the composites with the same lignin concentrations, the lignin with higher inorganic contents had lower viscosity. In previous studies, the presence of fillers increased viscosity of the composites.[18,20] Shumigin et al.[18] reported that cellulose filler increased the viscosity of PLA or PE matrix because a higher shear force is required to overcome stronger PLA–filler interaction. Shear thinning behaviors were often observed with fillers[21–23] due to stronger interaction between the polymers and fillers. Nagarajan *et al.*[20] suggested that the filler could induce the filler network or structural skeleton within the polymer matrix to raise the viscosity. However, they also found that adding nanoparticles or biochar with smaller particle sizes as filler reduced the viscosity of polymer composites despite that rigid particles are supposed to increase the viscosity because they cannot dissipate stress. In the present study, the viscosities of the composites were reduced by lignin addition, which could be due to lignin softening upon heating and its plasticizer effect. Also, hydrogen bonding between PLA molecules could be weakened due to the above described reactions between OHs in lignin fragments and PLA during the composite compounding. It is also expected that more lignin fragments were produced when the metal content in lignin was high. Accordingly, the flowability of the composite molecules was increased with the lignin with higher impurities.

Figure 3 shows complex viscosities of the composites as a function of temperature. Increasing temperature exponentially decreased viscosity of both PLA and PLA–lignin composites. The viscosities of the composites were lower than that of PLA at the entire tested temperature range, and the viscosity difference was more significant at lower temperatures. At 150 °C, the viscosity of PLA was 1741 Pa·s, whereas it reduced to 1004 Pa·s for PLA-L5, 825 Pa·s for PLA-M5, and 538 Pa·s for PLA-H5. Lower viscosities of the composite would allow the compounding at lower temperatures for energy saving.

Mechanical Properties. Mechanical properties of PLA and PLA–lignin composites are compared in Figure 4. The tensile strength of pure PLA was 52.46 MPa, and it decreased at the composites along with increasing lignin concentration. The decrease of tensile strength was also observed in the previous studies for PLA composites containing more than 5% of woody biomass lignin.[11,12] Tensile strength decreased in the composites, which is likely due to the incompatibility of PLA with lignin. Although PLA is a polyester, lignin is an aromatic polymer with a large amount of hydroxyls.[24] It has been reported that lignin can interrupt crystallinity of PLA, thus leading to a poor mechanical property.[25] From the figure, it is also evident that impurities in lignin affect the mechanical properties of the composites. For the composites with same lignin concentrations, PLA–M-lignin overall had better mechanical properties. The tensile strength of PLA-M5 was 48.39 MPa, which is 22.3% and 34.6% higher than the corresponding values of PLA-H5 and PLA-L5, respectively. When the present results were compared with literature results, it was found that the tensile strength of PLA-M5 was comparable or even higher than the PLA composites containing same amount of woody-biomass lignin fillers.[11,12] The fact that the lowest tensile strength was observed with PLA–L-lignin composites suggests that the presence of impurity metals was beneficial in improving tensile strength of the composites. Previously, Toriz *et al.* reported that polypropylene (PP) composite containing both lignin and common inorganic fillers (i.e., talc and mica) had higher tensile strength than the PP composite containing only lignin or the inorganic fillers.[26] They speculated that the combination

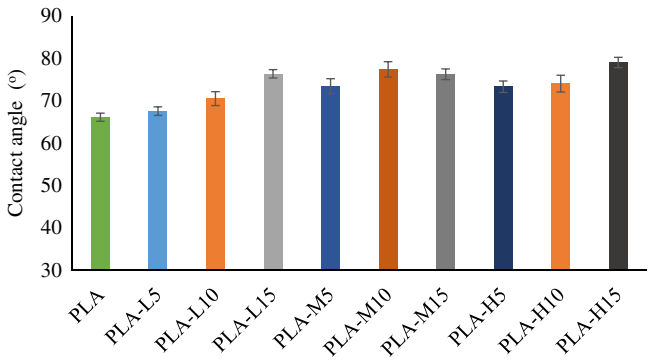

Figure 5. Contact angles of PLA and PLA–lignin composites. [Color figure can be viewed at wileyonlinelibrary.com]

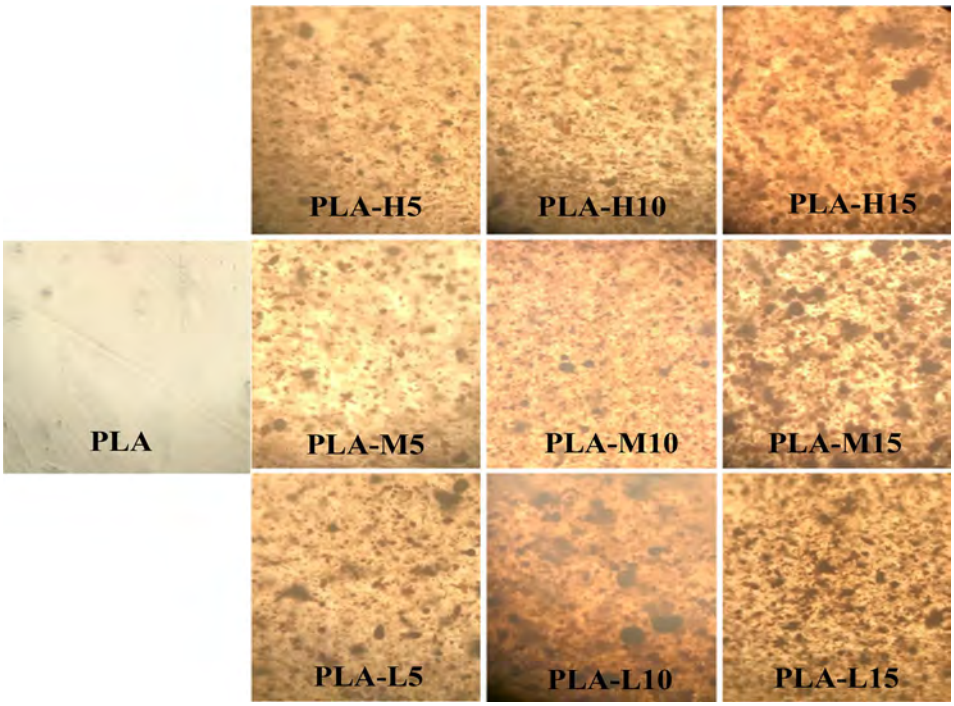

Figure 6. Optical micrographs of PLA and PLA–lignin composites. [Color figure can be viewed at wileyonlinelibrary.com]

of lignin and inorganic fillers improves particle distribution and the interaction between PP and fillers. However, no further insight could be provided. As described above, the catalytic effect of the metals promotes lignin fragmentation and could initiate the intermolecular reactions between PLA and the lignin fragments. Although it requires further investigation, such interactions may help to improve compatibility between PLA and lignin, therefore benefiting tensile strength of the composite. However, caution should be paid because using lignin filler with too high inorganic content is likely to have an adverse effect as the high content of impurity metals could degrade both lignin and PLA to lower tensile strength of the composites.

As also shown in Figure 4, the strain-at-break values of PLA–lignin composites were lower than that of pure PLA and decreased with increasing lignin concentration. The incompatibility of lignin in PLA matrix interrupted the ductility of PLA, leading to the increased brittleness of PLA–lignin composites. However, the strain was found to decrease least with PLA–M-lignin. For instance, the strain of PLA-M5 was 2.47%, 1.54% for PLA-L5, and 1.76% for PLA-H5. The strain of PLA–L-lignin was lowest. This result again shows the benefit of using the lignin with inorganic impurities for better compatibility between PLA and the filler.

From Figure 4, it can also be seen that PLA–lignin composites have higher modulus compared to pure PLA. This result is interesting because the use of woody biomass-derived lignin fillers lowered the modulus of PLA composites in previous studies.[11,12] In the present study, the modulus of PLA–H-lignin and PLA–L-lignin composites were similar. Both of them were not significantly affected by the lignin concentration in the composites. For PLA–M-lignin, a significant increase of the modulus was observed with PLA-M15. The increase of modulus could be attributed to the presence of inorganic impurities, as they can be acted as micro-rigid particles to prevent PLA macromolecules from deforming.[27] However, the results showed in this study imply that the modulus of the composites could be co-influenced by lignin and impurities content.

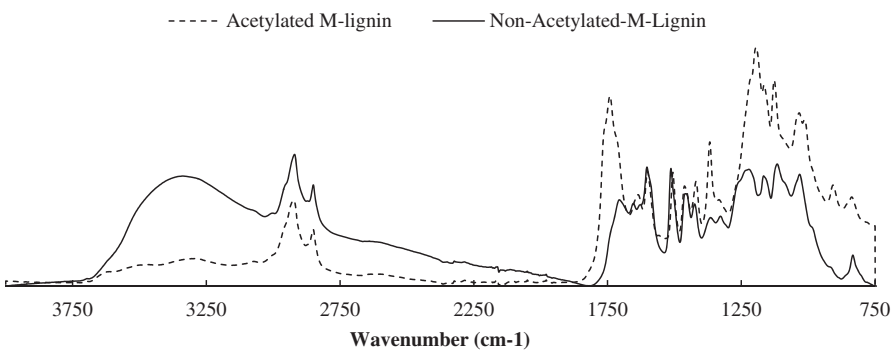

Figure 7. FTIR spectrum of M-lignin before and after acetylation.

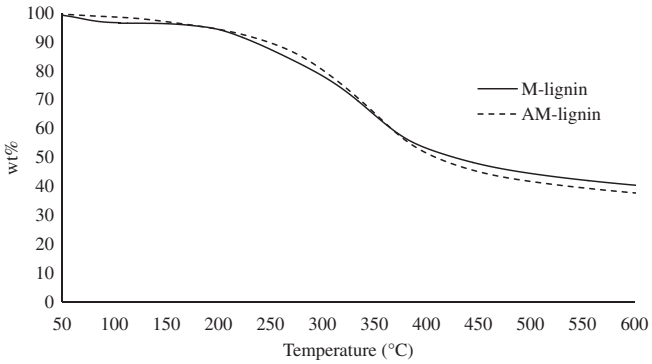

Figure 8. TGA curves of M-lignin before and after acetylation.

Table IV. Thermal Stability of PLA–AM-Lignin Composites

Composite	T_d (°C)	T_{max} (°C)
PLA-AM5	314.2	355.6
PLA-AM10	294.3	334.5
PLA-AM15	315.0	358.8

Contact Angle. The contact angles of the composites were measured, and the results are shown in Figure 5. The contact angle increased at PLA–lignin composites for their improved hydrophobicity. The similar phenomena were also observed with woody biomass-derived lignin fillers.[11,12] However, some variations were also observed in this study. Gordobil *et al.*[11] reported that the contact angle increases with increasing concentration of Kraft-lignin up to 5%. Further increasing the lignin concentration decreased the contact angle in their study. In the present study, the contact angle was found to increase with increasing filler concentration beyond 5%. It was also found that with same lignin concentration, the composites made with higher-impurity lignin in general had higher hydrophobicity. The possible reason could be the reduced hydrophilic OH groups in PLA. As described earlier, the end chain OHs in PLA could react with the OHs in lignin fragments to form aromatic C—O. The contact angle of PLA-L5 was only slightly higher than that of pure PLA, whereas it increased noticeably for both PLA-M5 and PLA-H5 because more lignin fragments were produced with higher impurity metals so that more OHs in PLA could be captured. Among PLA–M-lignin composites, PLA-M10 had the highest contact angle. Further increasing lignin concentration did not enhance hydrophobicity of the composite.

Optical Micrographics. The optical micrographics of PLA and PLA–lignin composites are shown in Figure 6. Although this analysis technique does not provide the information about the interaction between lignin and PLA at microscale like SEM technique does, it was effective in observing overall distribution of lignin fillers in PLA matrix in a broader area. As shown in the figures, the agglomerated lignin particles were distributed through the PLA matrix due to their immiscibility. In addition to the visible lignin particles, it was also noticed that the composite matrix appeared to be semitransparent light brown color compared to white color with pure PLA. This color change is likely due to homogeneous distribution of lignin particles with very small particle sizes (such as nano sized) or molecular bonding between PLA and lignin. This observation also indicates that there exists a low miscibility despite that lignin and PLA are largely immiscible. Interestingly, the amount of lignin agglomerates reduced in PLA–M-lignin and PLA–H-lignin in comparison to PLA–L-lignin for same lignin concentrations. This observation suggests the improved miscibility between lignin and PLA and thus supports our proposed theory that impurity metals present in lignin promote lignin fragmentations and softening to enhance the intermolecular reactions between lignin and PLA. The distributions of lignin fillers among PLA matrix were more homogenous in PLA–M-lignin compared to other composites. Better homogeneity of the composites is likely to promote higher tensile strength of the corresponding composites since discontinuity among the polymer matrix decreased and more integrated composite is formed. Among the composites with 10% lignin, PLA-L10 had the lowest tensile strength and the poorest homogeneity. The improved compatibility of PLA and the filler due to enhanced interaction between PLA and lignin fragments at molecular levels may explain why the presence of impurity metals can be helpful.

PLA and Acetylated M-Lignin Composites

From the above results, M-lignin provided best filler performance in terms of thermal stability, mechanical properties, and hydrophobicity. The higher properties of the composites are likely contributed by the improved compatibility between PLA and M-lignin. In this section, M-lignin was further acetylated and then blended with PLA. Acetylation is a common method to alter lignin properties and improve miscibility of lignin with other polymers.[28] Because the hydroxyls in lignin are substituted by acetyls, the inter and intra hydrogen bonding between lignin molecules was weakened by acetylation. As a result, acetylated lignin usually has much lower melting point and improved mobility.

Figure 9. Optical micrographics of PLA and acetylated M-lignin composites. [Color figure can be viewed at wileyonlinelibrary.com]

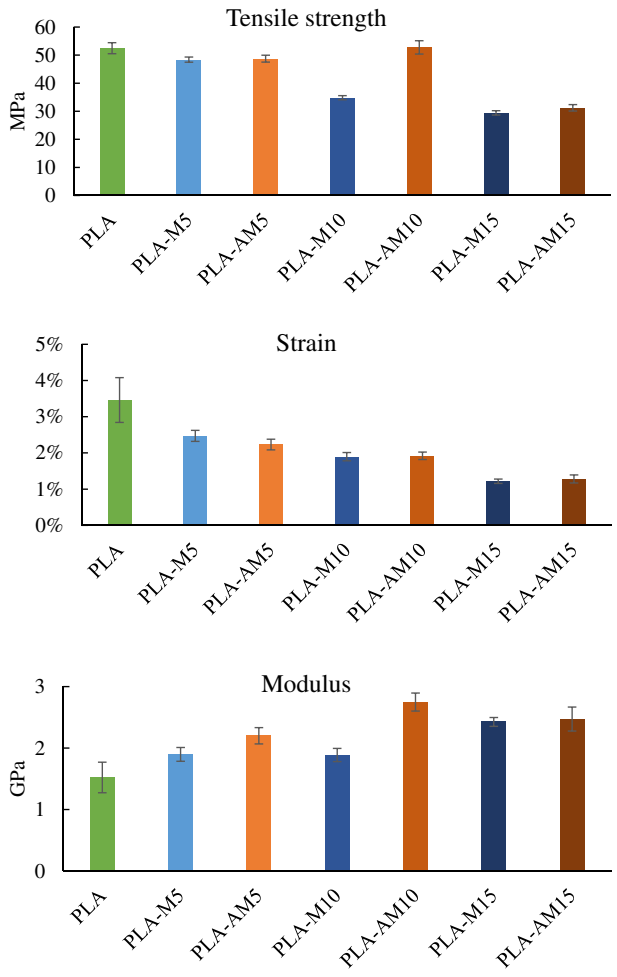

Figure 10. Mechanical properties of PLA, PLA–M-lignin, and PLA–AM-lignin composites. [Color figure can be viewed at wileyonlinelibrary.com]

The FTIR spectra of M-lignin before and after acetylation (AM-lignin) are compared in Figure 7. The spectrum of the M-lignin showed intense peaks at 3400 cm^{-1} for hydroxyls, 2900 cm^{-1} for C—H stretching, 1730 cm^{-1} for carbonyls, 1500 cm^{-1} for aromatic ring vibration, and 1230 cm^{-1} for esters. The peak appears at 1166 cm^{-1} is for ester stretch vibration, and the peak at 1030 cm^{-1} is for ether stretch and deformation. In the spectrum of the AM-lignin, the peak at 3400 cm^{-1} (for —OH) decreased significantly, whereas the peak at 1730 cm^{-1} (for C═O), 1365 cm^{-1} (for $—CH_3$), and 1230 cm^{-1} (for ester) increased dramatically. These changes confirmed that hydroxyl groups in M-lignin were successfully replaced by acetyl groups.

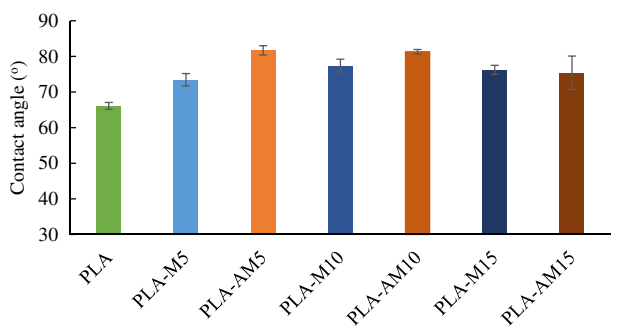

Figure 11. Contact angles of PLA, PLA–M-lignin composites, and PLA–AM-lignin composites. [Color figure can be viewed at wileyonlinelibrary.com]

The TGA profiles of M-lignin before and after acetylation are compared in Figure 8. Because the acetyl group is thermally stable at below 350 °C, the thermal stability of AM-lignin at the lower temperature region was enhanced. However, AM-lignin became more susceptive to decomposition at higher temperatures. The T_d and T_{max} values of the PLA-AM lignin composites are listed in Table IV.

Figure 9 shows optical micrographics of the PLA–AM-lignin composites. It could be seen that the miscibility of AM-lignin and PLA was significantly improved compared to that of the corresponding composites with non-acetylated lignin. Due to acetylation, polar hydroxyl groups in lignin was replaced by less-polar ester groups. Because ester groups are also abundant in PLA, the miscibility between acetylated lignin and PLA was improved.

The mechanical properties of PLA–AM-lignin compared with the corresponding properties of PLA–M-lignin are given in Figure 10. There was nearly no improvement in tensile strength for PLA-AM5 compared to PLA-M5 and PLA-AM15 compared to PLA-M15. However, tensile strength increased in PLA-AM10 to match that of pure PLA. This composite also had the most homogenous appearance due to the higher miscibility between PLA and the lignin.

Lignin acetylation had little influence on the strain of the composites. The strains of PLA-AM10 and PLA-AM15 were only slightly improved by acetylation. However, the modulus of the composites was further improved by acetylation. The maximum modulus of 2.75 GPa was achieved with PLA-AM10, for which the tensile strength was also highest.

Contact angles of the PLA–AM-lignin composites and PLA–M-lignin composites are compared in Figure 11. The contact angle of PLA-AM5 was 81.7°, higher than 73.4° with PLA-M5. Acetylated lignin is more hydrophobic since hydrophilic OH groups were replaced by less polar acetyl groups. However, the increase of hydrophobicity by acetylation was diminished when the lignin concentration increased to 15%. During the acetylation process, the inorganic content in M-lignin could be reduced. Thus, the decreased inorganic content in AM-lignin compared to M-lignin may also have played a role in the above observed changes in the properties.

CONCLUSIONS

In the present study, PLA–lignin composites were fabricated using corn stover derived organosolv lignin as the fillers. Overall, the use of lignin fillers improved thermal stability of the composites and reduced the complex viscosity. Compared to pure PLA, the PLA–lignin composites had decreased tensile strength but improved modulus and contact angles. The study also showed that the impurity metals remaining in unpurified lignin can significantly affect the properties of the composites. The presence of the impurity metals improved thermal stability of the composites at most of the cases, lowered the viscosity during compounding, and increased tensile strength and hydrophobicity of the composites. It is likely that the impurity metals catalyzed lignin fragmentations to promote the molecular interaction between lignin and PLA for better compatibility and reduced hydrophilic OH groups.

However, excessively high content of inorganic metals was also undesired as they can promote catalytic cracking to hinder thermal stability and mechanical properties of the composites. M-lignin was the optimum filler in terms of thermal stability and mechanical properties because it had better compatibility with PLA. Acetylating M-lignin further improved tensile strength and hydrophobicity of the composites. The tensile strength of PL-AM10 was similar to that of pure PLA, whereas the modulus increased to 2.75 GPa. Overall, this study examined the potential use of biorefinery originated, agricultural residue lignin as filler material, and further evaluated the possibility of using unpurified lignin to eliminate costly purification process.

ACKNOWLEDGMENTS

The authors like to acknowledge Dr. Yuan Xue, Dr. Patrick Johnston, and Ms. Chaoyue Huang at Iowa State University for their assistance during the research.

REFERENCES

1. Ragauskas, A. J.; Beckham, G. T.; Biddy, M. J.; Chandra, R.; Chen, F.; Davis, M. F.; Davison, B. H.; Dixon, R. A.; Gilna, P.; Keller, M. *Science*. **2014**, *344*, 1246843.
2. Ioannidou, O.; Zabaniotou, A. *Renew. Sustain. Energy Rev.* **2007**, *11*, 1966.
3. Luo, H.; Abu-Omar, M. M. *Green Chem.* **2018**, *20*, 745.
4. Qu, W.; Xue, Y.; Gao, Y.; Rover, M.; Bai, X. *Biomass Bioenergy*. **2016**, *95*, 19.
5. Effendi, A.; Gerhauser, H.; Bridgwater, A. V. *Renew. Sustain. Energy Rev.* **2008**, *12*, 2092.
6. Pucciariello, R.; Villani, V.; Bonini, C.; D'Auria, M.; Vetere, T. *Polymer*. **2004**, *45*, 4159.
7. Wu, L. C. F.; Glasser, W. G. *J. Appl. Polym. Sci.* **1984**, *29*, 1111.
8. Canetti, M.; Bertini, F.; De Chirico, A.; Audisio, G. *Polym. Degrad. Stab.* **2006**, *91*, 494.
9. Chen, F.; Dai, H.; Dong, X.; Yang, J.; Zhong, M. *Polym. Compos.* **2011**, *32*, 1019.
10. Baumberger, S.; Lapierre, C.; Monties, B.; Della Valle, G. *Polym. Degrad. Stab.* **1998**, *59*, 273.
11. Gordobil, O.; Delucis, R.; Egüés, I.; Labidi, J. *Indus. Crops Prod.* **2015**, *72*, 46.
12. Gordobil, O.; Egüés, I.; Llano-Ponte, R.; Labidi, J. *Polym. Degrad. Stab.* **2014**, *108*, 330.
13. Eom, I.-Y.; Kim, J.-Y.; Kim, T.-S.; Lee, S.-M.; Choi, D.; Choi, I.-G.; Choi, J.-W. *Bioresour. Technol.* **2012**, *104*, 687.
14. Berchem, T.; Roiseux, O.; Vanderghem, C.; Boisdenghien, A.; Foucart, G.; Richel, A. *Biofuels Bioprod. Biorefin.* **2017**, *11*, 430.
15. Zhou, S.; Xue, Y.; Sharma, A.; Bai, X. L. *ACS Sustainable Chem. Eng.* **2016**, *4*, 6608.
16. Hamzah, F.; Idris, A.; Shuan, T. K. *Biomass Bioenergy*. **2011**, *35*, 1055.
17. Patwardhan, P. R.; Satrio, J. A.; Brown, R. C.; Shanks, B. H. *Bioresour. Technol.* **2010**, *101*, 4646.
18. Shumigin, D.; Tarasova, E.; Krumme, A.; Meier, P. *Mater. Sci.* **2011**, *17*, 32.
19. Hamad, K.; Kaseem, M.; Deri, F. *Adv. Chem. Eng. Sci.* **2011**, *1*, 208.
20. Nagarajan, V.; Mohanty, A. K.; Misra, M. *ACS Omega*. **2016**, *1*, 636.
21. Pardo, S.; Bernal, C.; Ares, A.; Abad, M.; Cano, J. *Polym. Compos.* **2010**, *31*, 1722.
22. Lozano, K.; Bonilla-Rios, J.; Barrera, E. *J. Appl. Polym. Sci.* **2001**, *80*, 1162.
23. Marcovich, N. E.; Reboredo, M. M.; Kenny, J.; Aranguren, M. I. *Rheolog. Acta*. **2004**, *43*, 293.
24. Gellerstedt, G.; Henriksson, G. Monomers, Polymers and Composites from Renewable Resources; Elsevier: Oxford, United Kingdom, **2008**.
25. Spiridon, I.; Leluk, K.; Resmerita, A. M.; Darie, R. N. *Compos. Part B Eng.* **2015**, *69*, 342.
26. Toriz, G.; Denes, F.; Young, R. *Polym. Compos.* **2002**, *23*, 806.
27. Ho, M.; Lau, K.; Wang, H.; Hui, D. *Compos. Part B Eng.* **2015**, *81*, 14.
28. Qu, W.; Liu, J.; Xue, Y.; Wang, X.; Bai, X. *J. Appl. Polym. Sci.* **2018**, *135*, 45736.